International Journal of Fracture, Vol. 10, No. 2, June 1974
Noordhoff International Publishing – Leyden
Printed in The Netherlands

Slow crack growth in brittle materials under dynamic loading conditions

A. G. EVANS*

Materials Department, School of Engineering, University of California, Los Angeles 90024 *(U.S.A.)*

(Received January 25, 1973; in revised form May 7, 1973)

ABSTRACT

The failure of materials due to slow crack growth, under dynamic loading conditions, is analyzed in terms of crack velocity, stress intensity relationships. It is shown that this type of analysis can fully describe the failure characteristics for both constant strain-rate and constant stress-rate loading. The analysis is used to predict the variations of strength and subcritical crack growth with strain-rate and stress-rate. Application of the analysis to several ceramic systems give data which are entirely consistent with available experimental data.

1. Introduction

Recent studies have shown that slow crack growth in ceramic [1, 2] and brittle metallic [3, 4] systems can be described by the crack velocity (V) and the stress intensity factor (K) for a given microstructure and corrosive species (if required). The relationship between K and V for any system depends on the concentration of the corrosive species in the test environment and the test temperature; it is independent of crack length, test geometry, etc. Typical K, V curves are shown schematically in Fig. 1. There are three principal regions: Region I in which the rate of the reaction at the crack tip controls crack motion and in general, $V \propto \exp(\beta K)$, where β is a

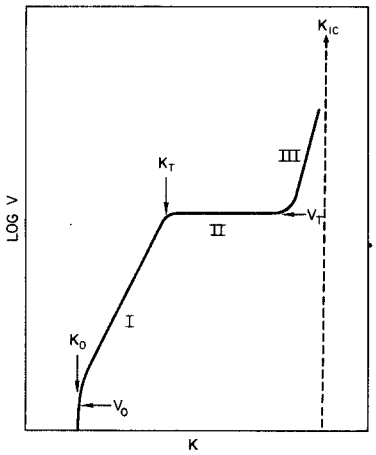

Figure 1. A schematic representation of a typical K, V curve. K_0 is the stress corrosion limit for the system and K_T is the stress intensity factor at the onset of Region II. V_0 is the velocity acquired by the crack when K reached K_0; V_T is the constant crack velocity in region II.

constant (this region commences at the minimum K value for the system, K_0, the slow crack growth limit) [2]; Region II in which the crack velocity is essentially constant and crack motion is controlled by diffusion of the corrosive species; Region III in which the crack velocity increases very rapidly with increase in K. At the onset of Region III, K is generally close to K_{IC}, the critical stress intensity factor for crack propagation in the absence of slow crack growth. It is usually possible, therefore, to consider that fast fracture ($K = K_{IC}$) commences at the end of region II [4]. As crack growth proceeds K continues to increase, due to the kinetic energy

* Now at: Inorganic Materials Division, National Bureau of Standards, Washington, D. C. 20234 (U.S.A.)

acquired by the specimen, but the rate of increase (dK/dV) is substantially lower than during slow crack growth.

Using K, V curves, it should be possible to predict any of the time dependent failure characteristics. It has already been shown [2, 4] that such curves can be used to successfully describe the variations in time-to-failure at constant applied tensile stress, σ. The curves have not, however, been used to examine the characteristics of dynamic failure at constant elastic strain-rate ($\dot{\varepsilon}$) or constant stress-rate ($\dot{\sigma}$). Constant strain-rate experiments are used extensively for fracture strength evaluations and it is important to understand how these strengths are affected by slow crack growth. A previous study by Charles [5] has examined constant stress-rate failure for a simplified K, V relationship. A more general description of dynamic failure (for both constant strain-rate and constant stress-rate loading) is presented in this paper based on the detailed form of the K, V curves.

First, the failure criteria for dynamic loading are defined and, based on these, a description of failure is derived from a typical K, V curve. This is followed by an examination of the effects of strain-rate and stress-rate on strength and on the crack extension that occurs prior to failure. Several specific systems are then examined so that the predicted description of failure may be compared with available experimental data.

2. Dynamic failure criteria

2.1. *Constant stress-rate failure*

For constant stress-rate the stress continues to increase until failure such that the maximum stress occurs just prior to the crack leaving the specimen. The maximum stress is thus found by relating stress σ, to the crack length, C, and hence obtaining σ at $C \approx W$, the specimen width.

2.2. *Constant strain-rate failure*

Constant strain-rate experiments are used extensively to obtain values of fracture strength (σ_f), i.e., the maximum stress during failure. In contrast to constant stress-rate experiments the fracture stress is generally reached well before the crack leaves the specimen. The condition for maximum stress is given quite simply by:

$$\left(\frac{\partial \sigma}{\partial C}\right)_{\dot{\varepsilon}} = 0 \tag{1}$$

The maximum stress is again found by relating stress and crack length, and then imposing the condition given by equation (1).

3. Stress crack length relations during slow crack growth

3.1. *Constant stress-rate conditions*

The stress intensity factor, K, is related to the stress by:

$$K = Y\sigma C^{\frac{1}{2}} \tag{2}$$

where Y is a geometrical factor that depends on C/W [6].

The crack velocity, dC/dt, is given by:

$$\frac{dC}{dt} = \left(\frac{\partial C}{\partial \sigma}\right)_{K,t} \frac{d\sigma}{dt}, \tag{3}$$

the other partial derivatives vanish for constant stress rate conditions because K is a unique function of V. Rearranging eqn. (3) gives

$$d\sigma = \frac{\dot{\sigma}}{V} dC \tag{4}$$

Since V is a function of K—and hence σ and C through eqn. (2)—this equation may be solved for σ, either numerically for each specific system, or analytically if there is a functional relationship between K and V. As described above, the K, V curves can be separated into three regions: in Region I, $V \propto \exp(\beta K)$; in Region II, V is approximately constant; then, at the end of region II, fast fracture occurs. It is convenient therefore to separate the integral into three K regimes.

In Region I, substitution of the exponential relationship between K and V into the integral leads to an intractable integration. A satisfactory solution to the integral requires therefore another relationship between K and V which also gives a good fit to the experimental data. It may be shown that a logarithmic relationship (of the type used by Charles [5]) in which V is proportional to K^n, *i.e.* $V/V_0 = (K/K_0)^n$ for $K > K_0$, usually gives as good a fit to available experimental data as the exponential relationship, for both metallic and ceramic systems (see Fig. 2 for the data on glass). The solutions to the integral are still however specific to a particular

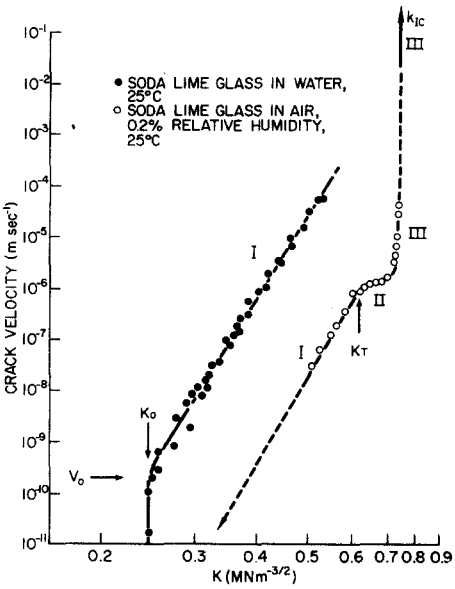

Figure 2. K, V data for the glass/water and glass/air (0.2% humidity) systems [2] plotted on logarithmic axes, showing that the data gives a very good fit in Region I to the relationship $V/V_0 = (K/K_0)^n$.

test geometry, unless $C \gtrsim 0.1\ W$ where Y is constant ($\approx \pi^{\frac{1}{2}}$). This simple solution, as shown later, applies to a large number of systems.

Substituting

$$V = V_0 \left(\frac{K}{K_0}\right)^n, \quad \text{and} \quad K = K_0 \left(\frac{C}{C_0}\right)^{\frac{1}{2}} \left(\frac{\sigma}{\sigma_0}\right)$$

into Eq. (4) and integrating gives*:

$$\sigma = \frac{K_0}{(\pi C_0)^{\frac{1}{2}}} \left[1 + \frac{2\dot{\sigma}\pi^{\frac{1}{2}}(n+1)C_0^{(n+1)/2}}{V_0 K_0 (n-2)} \left[\left(\frac{1}{C_0}\right)^{(n/2-1)} - \left(\frac{1}{C}\right)^{(n/2-1)}\right]^{1/(n+1)}\right] \tag{5}$$

except for $n=2$ where

$$\sigma = \frac{K_0}{(\pi C_0)^{\frac{1}{2}}} \left[1 + \frac{3\dot{\sigma}\pi^{\frac{1}{2}} C_0^{\frac{3}{2}}}{V_0 K_0} \ln\left(\frac{C}{C_0}\right)\right]^{\frac{1}{3}} \tag{6}$$

* Subscripts 0 in this paper refer to the value of the parameters corresponding to the initial extension of the crack.

When n is large, e.g., for glass (Fig. 2) $n=16$, σ rapidly approaches an asymptote of

$$\sigma = \frac{K_0}{(\pi C_0)^{\frac{1}{2}}}\left[1 + \frac{2\pi^{\frac{1}{2}}\dot{\sigma}\, C_0^{\frac{3}{2}}(n+1)}{V_0 K_0 (n-2)}\right]^{1/(n+1)} \tag{7}$$

In Region II, the analysis is similar but with $n=0$. Thus,

$$\sigma = \frac{K_T}{(\pi C_T)^{\frac{1}{2}}}\left[1 + \frac{\pi^{\frac{1}{2}}\dot{\sigma}\, C_T^{\frac{1}{2}}(C-C_T)}{V_T K_T}\right] \tag{8}$$

For subsequent crack growth, a modified form of equation (6) applies;

$$\sigma = \frac{K_{IC}}{(\pi C_{IC})^{\frac{1}{2}}}\left[1 + \frac{2\dot{\sigma}\pi^{\frac{1}{2}}(n+1)C_{IC}^{(n+1)/2}}{V_{IC}K_{IC}(n-2)}\left[\left(\frac{1}{C_{IC}}\right)^{(n/2-1)} - \left(\frac{1}{C}\right)^{(n/2-1)}\right]\right]^{1/(n+1)} \tag{9}$$

Since n is very large, this essentially reduces to:

$$\sigma = K_{IC}/(\pi C_{IC})^{\frac{1}{2}} \tag{10}$$

so that crack growth after region II occurs at constant stress. The nature of the stress, crack length variations described by equations (5 to 10) are depicted in fig. 3. A value for the fracture

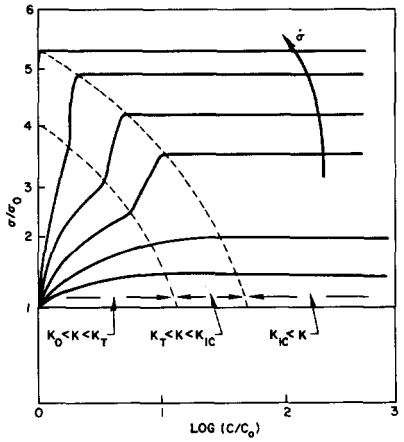

Figure 3. A schematic representation of the variation of stress with crack length for constant stress-rate experiments. The effects of increasing stress-rate ($\dot{\sigma}$) are indicated by the arrow.

stress, σ_f, is obtained from equations (5), (8), and (9), using $C=W$ as the fracture condition. This gives:

$$\sigma_f = \frac{K_0}{(\pi C_0)^{\frac{1}{2}}}\left[1 + \frac{2\pi^{\frac{1}{2}}\dot{\sigma}(n+1)C_0^{(n+1)/2}}{V_0 K_0 (n-2)}\left[\left(\frac{1}{C_0}\right)^{n/2-1} - \left(\frac{1}{C_T}\right)^{n/2-1}\right]\right]^{1/(n+1)}$$
$$\times\left[1 + \frac{\pi^{\frac{1}{2}}\dot{\sigma}\, C_T^{\frac{1}{2}}}{V_T K_T}(C_{IC}-C_T)\right] \tag{11}$$

(This is essentially the same as the stress at $K=K_{IC}$, so that for all practical purposes the fracture condition may be taken as the stress at which $K=K_{IC}$ rather than the stress at $C=W$). For relatively small $\dot{\sigma}$ and C_0, Eq. (11) reduces to,

$$\sigma_f = \frac{K_0}{(\pi C_0)^{\frac{1}{2}}}\left[1 + \frac{2\pi^{\frac{1}{2}}\dot{\sigma}(n+1)}{V_0 K_0 (n-2)}C_0^{\frac{3}{2}}\right]^{1/(n+1)} \tag{12}$$

which resembles the expression obtained by Charles [5], except at stresses approaching the stress corrosion limit.

For values of $C_{IC} > 0.1$ W, σ_f depends on the test geometry (through the Y factor) and each geometry must be analyzed separately using a numerical integration.

3.2. *Constant strain-rate conditions*

The analysis is developed on a similar basis to the constant stress-rate analysis, except that $\dot{\sigma}$ is replaced by an expression containing the strain-rate $\dot{\varepsilon}$. Stress and strain in a cracked body are related, via the elastic modulus (E), by:

$$\sigma = E\varepsilon f(C) \tag{13}$$

where $f(C)$ decreases as C increases and for a tensile experiment if may be shown that[7]:

$$f(C) = \frac{LW}{LW + 2\int Y^2 C\,dC} \tag{14}$$

where L is the gauge length.

Differentiating Eq. (13) with respect to time to introduce the strain-rate and substituting for $\dot{\sigma}$ in eq. (4) gives:

$$d\sigma = \left\{ Ef(C)\dot{\varepsilon} + \frac{\sigma}{f(C)}\left[\frac{df(C)}{dt}\right] \right\} \frac{dc}{V} \tag{15}$$

Again, if $C_{IC} < 0.1$ W so that $Y \approx \pi^{\frac{1}{2}}$ then $f(C) = f(C)_0 = 1$, and the integration is a general one. The solutions are identical to Eqs. (5 to 10) except that $\dot{\sigma}$ is replaced by $E\dot{\varepsilon}$. As crack growth proceeds, however, Y and $f(C)$ start to vary and the expressions for the stress should be

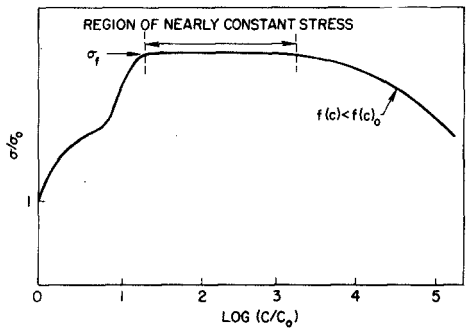

Figure 4. A schematic representation of the variation of stress with crack length for constant strain-rate experiments. The effects of loading rate are similar to those in Fig. 3 for constant stress-rate conditions.

multiplied by $Yf(C)/Y_0 f(C)_0$. The term $f(C)$ decreases at relatively large C/C_0—when there is a significant reduction in the stiffness of the test specimen—and then the stress starts to decrease, as shown schematically in Fig. 4. Apart from this effect at large C/C_0, the stress, crack length variations are identical for both constant stress-rate and constant strain-rate experiments, provided that $C_{IC} \gtrsim 0.2$ W (where $f(C) = f(C)_0 = 1$). For larger values of C_{IC}/W the integrations in Eqs. (4) and (15) are different and there are substantial differences throughout between the constant stress-rate and constant strain-rate curves.

The fracture stress may be obtained by superimposing the condition; $(d\sigma/dC) = 0$ at $\sigma = \sigma_f$. For $C_{IC} \leqslant 0.2$ W, $f(C) = f(C)_0 = 1$, and the maximum stress is reached during fast fracture. Then, the fracture stress is identical to the constant stress rate solution given by equation (11). If $C_{IC} > 0.2$ W, the constant strain-rate fracture stress will be less than the constant stress rate fracture stress, due to the reduction in $f(C)$ before C reaches C_{IC}.

A value for the crack length at the fracture stress, C_f, may be obtained by putting the condition,

$$\ln\left(\frac{K}{K_0}\right) = \tfrac{1}{2}\ln\left(\frac{C}{C_0}\right) + \ln\left(\frac{Y}{Y_0}\right),$$

into the fracture stress equation. This shows that (for a given C_0) $C_f/C_0 \approx 1$ at low strain-rate —where fracture occurs at σ_0—and then increases as the strain-rate increases. However, C_f/C_0 is also ≈ 1 at high strain-rates where fracture occurs as it would in the absence of a corrosive environment. C_f thus passes through a maximum at intermediate strain-rates. (The magnitude of the maximum in C_f depends on Y and $f(C)$, and hence upon the test geometry). Conversely C_{IC} is a maximum at low strain-rates and decreases to C_0 at high strain-rates. This means that, at low strain-rates, the fracture stress is reached for crack lengths substantially smaller than C_{IC}, whereas for larger strain-rates the fracture stress essentially coincides with $C = C_{IC}$. The fracture stress in a constant strain-rate experiment is not therefore, determined, in general, by the stress at which $C = C_{IC}$ (or $K = K_{IC}$).

The importance of K_{IC} emerges when the variation with time of stress, crack length, etc. is examined. When $K > K_{IC}$ the crack velocity increases sharply with crack length, so that the crack length—and hence the stress—vary rapidly with time. C_{IC} is therefore a more useful crack-length parameter than C_f, because it corresponds to the maximum crack extension prior to *a rapid* decrease in load and, for practical purposes, it also corresponds to the maximum crack extension that can be achieved before load removal no longer prevents failure. C_{IC} may therefore be regarded as the limit of stable crack growth.

4. Effects of loading rate on the fracture parameters

The effect of strain-rate on strength is shown schematically in Fig. 5. There is a maximum of four regions A, B, B′ and D. At low strain-rates, Region A, the strength begins to increase from

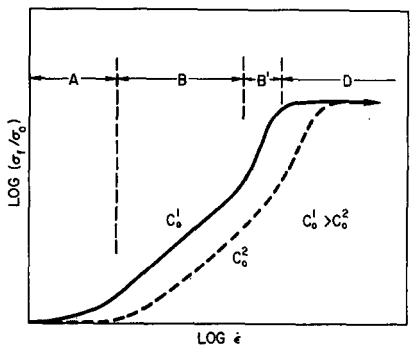

Figure 5. A schematic representation of the effects of strain-rate on strength.

the minimum value for the system, σ_0. At higher strain-rates, Region B, there is a simple logarithmic relationship between σ_f and $\dot{\epsilon}$, *i.e.*, $\log \sigma_f \propto 1/(n+1) \log \dot{\epsilon}$; this region occurs if n is relatively large and its extent depends upon the K range for Region I of the K, V curve (K_T/K_0). At still higher strain-rates, Region B′, strength varies in a complex manner with strain-rate; this region occurs if K reaches K_T before entering the "region of nearly constant" stress in Fig. 4, and its extent depends on the K range for region II (K_{IC}/K_T). Finally, at the highest strain-rates, Region D, fracture occurs at a stress approaching that expected in the absence of slow crack growth. (The effects of stress-rate on strength are similar, although the absolute strengths may differ if $C_{IC} > 0.2$ W).

The sub-critical crack extension, C_{IC}, also varies with loading rate over the same range of strain-rates (stress-rates) as σ_f. There are again four regions of behavior with C_{IC} decreasing from a maximum value at low strain-rates to C_0 at high strain-rates.

This general analysis of failure under dynamic loading should now be applied to a specific system to enable the analytical data to be compared with available experimental data. The only systems for which reliable K, V and σ_f, $\dot{\epsilon}$ data are available for comparable materials and testing conditions are soda-lime glass and polycrystalline aluminum oxide in water-containing environments; these systems are considered in the following section.

5. Dynamic failure of glass and alumina in water containing environments

The stress intensity, crack velocity curves for soda-lime glass and alumina in two water concentrations at 25°C are shown in Figs. 2 and 6. A lower limit for $K(K_0)$ is detected for the tests on glass in water, at 0.25 MN $m^{-\frac{3}{2}}$, with a corresponding V_0 of 3×10^{-10} m sec^{-1}. The slope of the curves in Region I give n values of 16 and 31 for glass and alumina respectively. The corresponding values for K_{IC} are 0.75 MN $m^{-\frac{3}{2}}$ [8] and 5.4 MN $m^{-\frac{3}{2}}$ [9, 12].

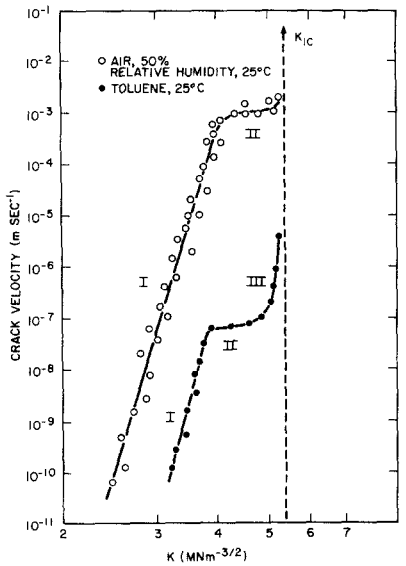

Figure 6. K, V data for the alumina/air system [8].

The strain-rate dependence of strength can be calculated from the K, V curves, using equation (11), for any value of the initial crack length C_0. If K_0 is not available, it can be shown by substitution in equation (11) that in minimum K obtained for the system—and the corresponding V—may be used without substantially affecting the solution, except at very low strain-rates. A comparison with existing strength data requires, therefore, that a value for C_0 should be available. The dimensions of pre-existing cracks in ceramic materials are not readily amenable to empirical evaluation, so that C_0 values are not normally available. It is expedient, therefore, to calculate C_0 from the strength and then to use this C_0 to generate the strength, strain-rate relationship. The analysis thus affords comparisons of relative strength variations.

A comparison of strength variations obtained on abraded glass—pre-existing flaw size ~ 10 μm—with the predicted variation is shown in fig. 7. Although the data is limited, the agreement is good. Also included in fig. 7 are the effects of strain-rate on strength for glass containing larger, 50 μm, or smaller, 2 μm, flaws. It is noticed that an increase in flaw size reduces the strength, as expected, but also translates the strain-rate dependent strength regime to lower strain-rates.

A similar comparison for alumina is shown in fig. 8. Here there is very good agreement between the predicted curves and the experimental data for both notched and unnotched bars. The notched bar curve was calculated directly from equation (11) because a C_0 value was available. This comparison thus provides confirmation of the absolute predictions of equation (11), whereas verification of relative strength predictions is provided by the other data.

Finally, it is interesting to note that the strength variation at fixed strain-rate—due to the range of pre-existing flaw sizes—is smaller when slow crack growth occurs than in the absence of slow crack growth (fig. 9). For example, the 2 μ variation in strength for abraded glass rods in the absence of water (fig. 9) is from 100 to 200 MN m^{-2} (150 MN m^{-2} mean), whereas the

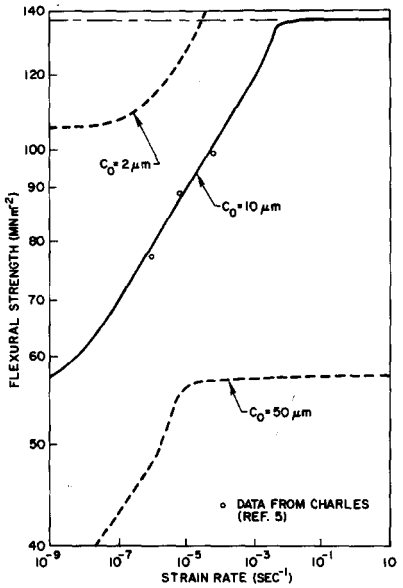

Figure 7. A comparison of the predicted effects of strain-rate on strength, for abraded glass, with experimental data [5].

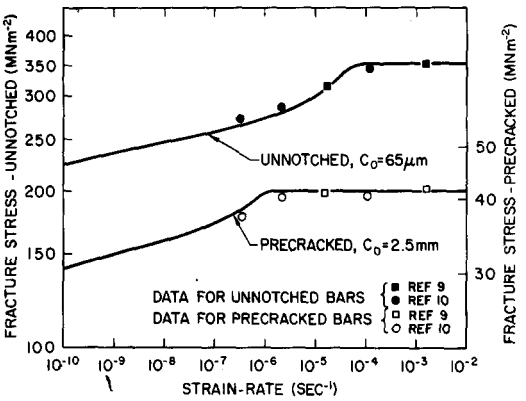

Figure 8. A comparison of the predicted effects of strain-rate on strength, for polycrystalline alumina, with experimental data [9, 10].

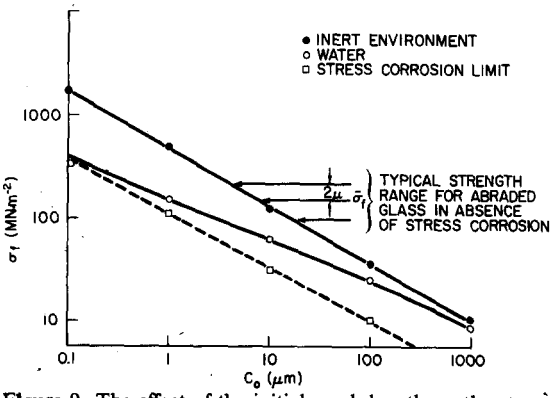

Figure 9. The effect of the initial crack length on the strength of glass in water at a strain-rate of 10^{-5} sec^{-1}.

strength of the same rods tested in water varies from 66 MN m^{-2} to only 90 MN m^{-2} (75 MN m^{-2} mean).

It is concluded, therefore, that there is a very good correlation between predicted strength, strain-rate variations and available data for materials containing relatively large pre-existing flaws, where fracture is determined exclusively be the extension of these flaws. If a flaw initiation stage is required, this will modify the strength, strain-rate relationship and some additional information about flaw initiation is required to enable strengths to be predicted. (A flaw initiation stage appears to be required in chemically polished glass, so that the relative strength variations predicted using equation (11), are not in good agreement with the measured strength variations [11]).

6. Conclusion

An analysis for predicting stress, crack length variations from crack velocity, stress intensity diagrams, under both constant strain-rate and constant stress-rate loading, is presented. The effects of strain-rate and stress-rate on strength are then obtained by incorporating the appropriate failure criteria.

The predicted strength, strain-rate variations are in good agreement with measured effects when failure is controlled exclusively by the propagation of pre-existing flaws. When a flaw initiation stage is required, additional information about the kinetics of flaw initiation are needed for strength predictions.

REFERENCES

[1] S. M. Wiederhorn, *J. Am. Ceram. Soc.*, 50 (1967) 407.
[2] S. M. Wiederhorn and L. H. Bolz, *J. Am. Ceram. Soc.*, 53 (1970) 543.
[3] H. G. Nelson, A. S. Tetelman and D. P. Williams, *Proceedings of the International Conference on Corrosion Fatigue*, Storrs, Connecticut June 1971.
[4] D. P. Williams, *Internl. Jnl. Frac. Mech.*, to be published.
[5] R. J. Charles, *J. Appl. Phys.*, 29 (1958) 1657.
[6] W. F. Brown and J. E. Srawley, *ASTM, STP* 410 (1967).
[7] See for example, J. P. Berry, *J. Mech. Phys. Solids*, 8 (1960) 194.
[8] S. M. Wiederhorn, *J. Am. Ceram. Soc.*, 52 (1969) 99.
[9] R. W. Davidge and G. Tappin, *Proc. Brit. Ceram. Soc.*, 15 (1970) 47.
[10] A. G. Evans, unpublished results.
[11] J. E. Ritter and C. L. Sherburne, *J. Am. Ceram. Soc.*, 54 (1971) 601.
[12] A. G. Evans, *Internl. Jnl. Frac. Mech.*, to be published.

RÉSUMÉ

La rupture des matériaux due à une propagation lente d'une fissure sous des charges dynamiques est analysée en termes de relations entre la vitesse de propagation et l'intensité des contraintes.

On montre que le type d'analyse envisagé peut complètement décrire les caractéristiques d'une rupture sous charges caracterisées par une vitesse constante de déformation, ou par une vitesse constante de tension.

On utilise l'analyse pour prédire les variations de la résistance et la propagation subcritique de la fissure en fonction de la vitesse de déformation ou de mise sous tension.

L'application de l'analyse à divers systèmes céramiques fournit des données qui satisfont entièrement les données expérimentales disponibles.

ZUSAMMENFASSUNG

Der Bruch von Material durch langsame Rißausdehnung, unter dynamischer Beanspruchung wird in Hinsicht der Beziehung zwischen der Rißausdehnungsgeschwindigkeit und der Spannungsintensität untersucht. Man zeigt daß diese Form von Untersuchung die Bruchbegebenheiten vollständig beschreiben kann sowohl für eine Belastung, sowohl unter konstantem Verformungsgrad, als unter konstantem Spannungsgrad. Die Untersuchung wird zur Voraussagung der Änderungen der Festigkeit und des subkritischen Rißwachstums mit dem Verformungs- und dem Spannungsgrad. Die Anwendung der Untersuchung auf verschiedene Keramiksysteme ergibt Ergebnisse die vorzüglich mit bestehenden Versuchsergebnissen übereinstimmen.